

**Supplementary Design and Methods** Primers for fluorescent fragment PCR (FF-PCR) and sanger sequencing (forward primer indicated first)

Locus	FF-PCR	Sanger
NR21	TAAATGTATGTCTCCCCTGG Hex-ATTCTACTCCGCATTCACA	
NR22	GAGGCTTGTCAAGGACATAA Fam-AATTCGGATGCCATCCAGTT	
NR24	CCATTGCTGAATTTTACCTC Hex-GAGGCTTGTCAAGGACATAA	
BAT25	Tmr-TCGCCTCCAAGAATGTAAGT TCTGCATTTTAACTATGGCTC	
BAT26	AACCATTCAACATTTTAAACC Fam-TGACTACTTTTACTTCAGCC	
MONO27	TTGCAGTGAGCTGAGATTGC Fam-GGTGGATCAAATTTCACTTGG	
ATR	ACGGACATGTGGACCTCTTC TCACTCACCAAGTTTTACTGGA	TCTTCTCCGTGAGTCCTGT CTGAGGAAGAGCAGCCCATA
ATM	AAATCCTTTTTCTGTATGGGAT GTTACTGAGTCTAAAACATGG	CTCAGCAACAGTGGTTAG GATATGATTTAGACCTGAAGAG
BLM	CTCTGCCACCAGGAAGAATC CAGCAGTGCTTGTGAGAACA	CTCTGCCACCAGGAAGAATC GGAAGATTTGCTGGCTGCTA
CHK1	ATGGGACCAACCCAGTGAC TCCAAGAAATCGGTACTCTTTCA	CCTCCCAAAGTGCTGTGATT TCCAAGAAATCGGTACTCTTTCA
CtIP	TTGTCCCCTTCTCTTTTACAGC CCCAAGACTGTGATGTGTGAA	TTGTCCCCTTCTCTTTTACAGC GGGGCAGCTTACTTCATGTT
DNA-PKcs	TGGAGCAATGATGTAAGAGCTG AAATAGCAGGCTGTGCCAGT	
BRCA1	CAGGTTTAATATCCACTTTG ATTAGTTCTGATTTTGGTC	
BRCA2 Exon 9	GATACAGAATTTATCATCTTG CTGAAAATTACAATGAAAGG	
BRCA2 Exon 22	GATACAGAATTTATCATCTTG CTGAAAATTACAATGAAAGG	
MRE11	TGGAGGAGAATCTTAGGGAAAA AATTGAAATGTTGAGGTTGCC	TTGAAATGAATTGTCGCCTATG AATTGAAATGTTGAGGTTGCC
PTEN	AGTTCCTCAGCCGTTACCT TTTTGGATATTTCTCCAATGAA	TGCAGATCCTCAGTTTGTGG GCCATAAGGCCTTTTCCTTC
PARP1	CGCACATCTTGTCCCCTTGG GGCCCTCACCTTCTCCTTG	
TNK1	AACCATTGTTTCATTGACA AATCTTACCAGTGCTGTTTC	
RAD50	TGCGACTTGCTCCAGATAAA GCTACATGTACAGTGAAGGTAAATCC	CTCTGCCACCAGGAAGAATC GGAAGATTTGCTGGCTGCTA
TGF-βII	CAAGCTCCCCTACCATGACT TGCACTCATCAGAGCTACAGG	

**TP53 sequencing** *TP53* (NC\_000017-9) mutations were analyzed from DNA using the Roche GS FLX sequencing platform (Roche, Indianapolis, IN) as described previously<sup>1</sup>. We sequenced 14 amplicons for 95 samples across the entire *TP53* coding region and untranslated exon 1. Patient-specific barcodes, adapted to polymerase chain reaction primers in the second round of amplification were derived from the Roche GS Titanium protocol (Roche). Average sequencing coverage across *TP53* was around 1,200x and > 99% of the sequenced amplicons had sequence coverage of > 100x. This allowed reliable detection of mutant clones down to 1% to 2% relative mutation abundance (RMA), defined as the proportion of sequence reads containing the mutation. Independent polymerase chain reaction and GS FLX sequencing experiments were performed for confirmation of mutations in all cases (giving > 2,000x total coverage on average across a given mutation). These experiments also negated sampling errors for RMA calculations that were due to a higher combined sequencing coverage. Sanger sequencing confirmation was performed in a selection of patients where the mutation had an RMA of  $\geq 25\%$ . To determine the presence of low-abundance mutant clones, two samples were re-sequenced at greater depth (2,500x v 1,200x).

p53promoterA\_F GTAGTGCGATGGCCAGTCAGAGTGATAAGGGTTGTGAAGG  
p53promoterA\_R CAGTGTGCAGCGATGACCTGGCACAAAGCTGGACAGT  
p53promoterB/exoF GTAGTGCGATGGCCAGTGGCGGATTACTTGCCCTTAC  
p53promoterB/exoR CAGTGTGCAGCGATGACCGAGAGCCCGTGACTCAG  
p53exon2\_F GTAGTGCGATGGCCAGTCTGGATCCCCACTTTTCCTC  
p53exon2\_R CAGTGTGCAGCGATGACTCCCACAGGTCTCTGCTAGG  
p53exon3\_F GTAGTGCGATGGCCAGTAGCGAAAATTCATGGGACTG  
p53exon3\_R CAGTGTGCAGCGATGACGGGGACTGTAGATGGGTGAA  
p53exon4A\_F GTAGTGCGATGGCCAGTCCTGGTCCTCTGACTGCTCT  
p53exon4A\_R CAGTGTGCAGCGATGACTTCTGGGAAGGGACAGAAGA  
p53exon4B\_F GTAGTGCGATGGCCAGTGTCCAGATGAAGCTCCCAGA  
p53exon4B\_R CAGTGTGCAGCGATGACCAGGCATTGAAGTCTCATGG  
p53exon5\_F GTAGTGCGATGGCCAGTTTTCAACTCTGTCTCCTTCCTCTT  
p53exon5\_R CAGTGTGCAGCGATGACAGCCCTGTCGTCTCTCCAG  
p53exon6\_F GTAGTGCGATGGCCAGTCAGGCCTCTGATTCCTCACT  
p53exon6\_R CAGTGTGCAGCGATGACCTTAACCCCTCCTCCCAGAG  
p53exon7\_F GTAGTGCGATGGCCAGTTCATCTTGGGCCTGTGTTATC  
p53exon7\_R CAGTGTGCAGCGATGACAGTGTGCAGGGTGGCAAG  
p53exon8\_F GTAGTGCGATGGCCAGTGCCTCTTGCTTCTCTTTTCC  
p53exon8\_R CAGTGTGCAGCGATGACTAACTGCACCCTTGGTCTCC  
p53exon9\_F GTAGTGCGATGGCCAGTGGAGACCAAGGGTGCAGTTA  
p53exon9\_R CAGTGTGCAGCGATGACGAAAACGGCATTGAGTGT  
p53exon10\_F GTAGTGCGATGGCCAGTACTTCTCCCCCTCCTCTGTT  
p53exon10\_R CAGTGTGCAGCGATGACGAAGGCAGGATGAGAATGGA  
p53exon11\_F GTAGTGCGATGGCCAGTTGTCATCTCTCCTCCCTGCT

p53exon11\_R CAGTGTGCAGCGATGACCAAGGGTTCAAAGACCCAAA  
 p53extraexons\_F GTAGTGCGATGGCCAGTAACTTCAGAACACCAACTTATACCA  
 p53extraexons\_R CAGTGTGCAGCGATGACAGGTGTATTAATCCATTTTCAACTT

**Cell Culture** The leukemic cell lines; HL60, K562, NB4, U937, KG-1, Raji, Molm-13 and SD-1 cells were obtained from the American Type Culture Collection (ATCC). The colon cancer cell lines: DLD-1, LoVo, HCT116 and the leukemic cell lines, OCI-AML3, REH, OCI-AML3 were obtained from the DSMZ, Braunschweig, Germany. The myelomonocytic/myelodysplastic cell line, P39 was kindly donated by Richard Darley, (University of Wales, Cardiff, UK). Retrovirally immortalized PD220Di (human FANCD2<sup>-/-</sup>) was purchased from the Coriell Institute for Medical Research, Camden, NJ, USA. These cell lines were purchased within the last five years, propagated, expanded, and frozen immediately into numerous aliquots after arrival. The cells revived from the frozen stock were used within 10–20 passages, not exceeding a period of 2–3 months. The ATCC and DSMZ use morphological, cytogenetic and DNA profile analysis for characterization of cell lines. Prior to the study start, all MDS/AML cell lines were subjected to genotyping and mutation analysis for authenticity compared to the genotype characterised by the ATCC and DSMZ. Leukemic cell lines were cultured at 37°C (5% CO<sub>2</sub>) in Dutch-modified, RPMI 1640 medium, supplemented with 10% fetal calf serum, 4mM glutamine and 1% penicillin/streptomycin (all purchased from Sigma-Aldrich Co. Ltd. Poole, UK). Colon cancer cell lines were cultured in Dulbecco's minimal essential medium (DMEM) supplemented with 10% (v/v) fetal calf serum, 4mM glutamine and 1% penicillin/streptomycin. All cell lines were early passaged (between 10-20 passages). Peripheral blood lymphocytes (PBL) from unnamed normal subjects were prepared from heparinized blood using Hypaque-Ficoll (Sigma) gradients and cultured at 1 x 10<sup>6</sup> cells/ml in RPMI 1640, supplemented with 10% (v/v) fetal calf serum, 4mM glutamine and 1% penicillin/streptomycin. PBL were stimulated by adding phytohemagglutinin (PHA, Sigma) for 48 h, washed several times to remove PHA and then cultured in 1U/ml of Interleukin-2 (IL-2) for a maximum of 14 days. For primary cell cultures, bone marrow aspirates were taken from AML patients. Mononuclear cells were extracted using Hypaque-Ficoll (Sigma) gradients and cultured at 1 x 10<sup>6</sup> cells/ml in RPMI 1640, supplemented with 20% (v/v) fetal calf serum, 4 mM glutamine, 1% penicillin/streptomycin, 10 ng/ml IL-3, 10 ng/ml IL-6 and 20 ng/ml stem cell factor (SCF). DNA was extracted from cell lines and from primary cells using the QIAamp DNA Blood Mini Kit (Qiagen).

**Single nucleotide polymorphism analysis (SNP-A)** High quality genomic DNA was digested with NspI and Styl restriction endonucleases, followed by ligation to an enzyme specific adaptor. The ligated product was amplified by PCR, fragmented and end labelled with biotin. The labelled product was then hybridized to a SNP6 microarray. The Affymetrix 450 fluidics station and the Affymetrix 3000 G7 gene scanner were used to wash, stain, and scan the arrays. Arrays were quality checked to achieve a CpC score

>1.7/batch and a MAPD of <0.3 and were genotyped using the Affymetrix Genotyping Console with the Birdseed v2.0 algorithm. The base line reference for copy number data was derived from a cohort of 91 normal controls consisting of cases from the Medical Clinics at King's College London, as well as by external, publicly available data. Significant genomic changes were identified by size selection and by overlap with known copy number variants obtained from the Database of Genomic Variants (DGV). Deletions >270Kb, gains >500Kb and copy neutral LOH (CN-LOH)/uniparental disomy (UPD) >6.9Mb with <50% overlap with copy number variations from the DGV were considered to be somatic aberrations and were included in the analysis. Loss of heterozygosity was analyzed with the Copy Number Analyzer for the Affymetrix GeneChip Mapping (CNAG ver 3.0) algorithm and the Partek software. We confirmed allele specific analysis, somatic abnormalities and also detection of homozygous regions of deletions by the parallel analysis of buccal DNA from the same individuals.

**Sanger Sequencing** PCR reactions contained 100 nM primer in Amplitaq 360 taq polymerase/buffer and 10 ng of DNA. PCR was performed using the following conditions: denaturation at 94°C for 10 min, 35 cycles of denaturation 94°C for 30 sec, annealing at 55°C for 30 sec and extension at 72°C for 30 sec. There was a final extension step of 72°C for 7 min. PCR products were gel excised and DNA extracted. Sequencing was performed using Big dye (ABI) as per manufacturer's instructions.

**Cell cycle analysis** PARPi were added to log phase cells. At 120 h after PARPi addition, aliquots of  $2 \times 10^5$  cells were taken and centrifuged at 400 g for 10 min. The supernatant was aspirated and then 70% (v/v) ethanol (at -20° C) was added to the cells and gently vortexed. The cell suspension was again centrifuged at 400xg for 10 min. The supernatant was aspirated and then 1 ml of staining solution (PBS plus 5 ng FITC, 40 µg propidium iodide, 500 µg RNase) was added. Samples were analyzed using the FACScan flow cytometer (Becton Dickinson, Franklin Lakes, NJ). Calculating the percentage sub-G<sub>1</sub> events as a fraction of the total events derived the apoptotic index.

**PARP activity assay** MDS/AML cells were assessed for their intrinsic PARP activity by measuring the amount of poly(ADP-ribose) (PAR) synthesised by maximally stimulated PARP in a 6 min reaction, using a validated PARP activity assay<sup>2</sup>. Briefly, cells were washed in ice-cold PBS before permeabilising with digitonin (0.15 mg/mL, Sigma Aldrich, Dorset, UK). Confirmation of cell permeabilisation, and cell counting was performed using a haemocytometer following trypan blue staining. A known number of cells in reaction buffer (100 mM Tris-HCl, 120 mM MgCl<sub>2</sub>, pH 7.8) were then exposed to blunt-ended oligonucleotide (10 µg/mL, 5' CGGAATTCCG 3') (Europrim, Invitrogen, Paisley, UK) in the presence of NAD<sup>+</sup> (350 µM, Sigma Aldrich,) at a final volume of 100 µl for 6 min at 26°C. Cells were then fixed onto a nitrocellulose membrane (Hybond-N, Amersham, GE Healthcare Life Sciences, Bucks, UK) and PAR detected using the mouse monoclonal anti-PAR 10H antibody (1.5 mg/mL, Prof. Alex Burkle, University Konstanz, Konstanz, Germany). Anti-PAR antibody was detected by using the goat polyclonal horseradish peroxidase-conjugated anti-mouse antibody (DAKO, Cambridgeshire, UK). Antibodies were diluted at a concentration of 1:1000 in blocking

buffer (phosphate-buffered saline, 0.05 % Tween 20 and 5 % milk powder). Final detection of the secondary antibody was carried out by developing with ECL detection fluid (Amersham) and chemiluminescent detection using the Fujifilm LAS 300 imager (Raytest, Sheffield, UK). PARP activity of untreated control cells was set as 100 % and activity in all PARPi treated samples was expressed as a percentage of these cells activity.

**Comparison of PARPi** Abrogation of PARP activity was quantified using a modified version of the PARP Universal Colorimetric Assay Kit (R & D Systems Ltd, Abingdon, UK). This assay measures the incorporation of biotinylated ADP-ribose onto histone proteins bound to a 96-well plate. Detection is made by streptavidin conjugated HRP, followed by the addition of an HRP substrate. In this case, nuclear extract from the MDS/AML cell line, U937 was used as a source of PARP enzyme. Increasing concentrations of different PARPi were incubated with the U937 cells in culture before nuclear extracts were prepared and tested for PARP activity.

**Annexin V staining** Annexin V staining by FACS analysis was used as a marker of apoptosis. Five days (120 h) after PARPi exposure, cells were incubated with anti-annexin V-FITC and propidium iodide and analyzed by FACS immediately. Using Annexin V-FITC (FL-1, X-axis) and propidium iodide (PI) (FL-2, Y-axis), the percentage of non-apoptotic (bottom left quadrant), early (bottom right quadrant) and late apoptotic cells (top right quadrant) could be determined.

**ELISA** The method is based on the protocol provided by Abcam (Cambridge, UK). 2 X 10<sup>6</sup> cells were aspirated and washed in ice-cold PBS before lysis in extraction buffer (100 mM Tris, pH 7.4, 1 mM EGTA, 150 mM NaCl, 1 mM EDTA, 1% Triton X-100, 0.5% Sodium deoxycholate). Typically protein concentration was between 1-2mg/ml. All extracts were adjusted to 1mg/ml before assay. 100µl of cell extract was added to the wells of a 96 well plate and incubated at 4°C overnight. The extracts were washed 3 times with 200 µl PBS. The plates were then blocked in 200 µl blocking buffer, (5% non-fat dry milk or 5% serum in /PBS, per well) for 1 h. Then 100 µl of diluted primary antibody (1:50 for CtIP) was added to each well and incubated overnight at 4°C. The plates were again washed in PBS X5, before the addition of 100 µl of goat anti-rabbit IgG-HRP secondary antibody, diluted 1:1000) and incubated for 2h at at room temperature. The plates were then washed four times in PBS. Detection was made by the addition of 50 µl TMB (3,3',5,5'-tetramethylbenzidine) for 15-30 min and adding an equal volume of stopping solution (2 M H<sub>2</sub>SO<sub>4</sub>) before reading the optical density at 450 nm. A standard curve was prepared of relative absorbance vs protein concentration dependent on increasing concentration of si-RNA.

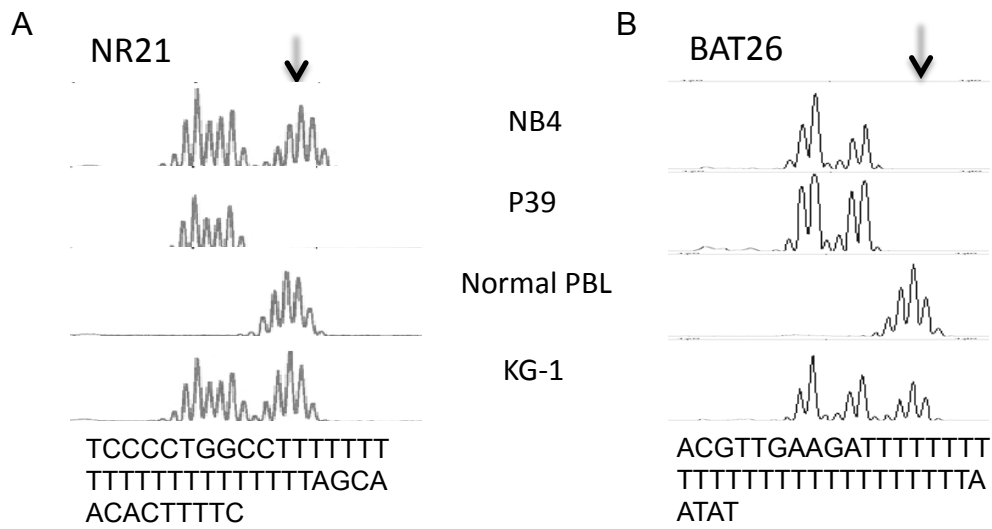
**Gene expression profiling** Total RNA was extracted from K562 cells transfected with Si-RNA targeted to CtIP, K562 transfected with CtIP over-expressing plasmid, pZGFP-C1-CtIP or Si-RNA scrambled oligonucleotide control using a hybrid TRIZOL (Invitrogen)/RNeasy (Qiagen) method. Briefly, cells were lysed and homogenized in 1 ml Trizol at room temperature for 5 min followed by phase separation by addition of 200 µl of chloroform. The aqueous phase was collected and an equal volume of 70% ethanol added, followed by application of this mixture to an RNeasy column. Subsequent steps

were according to manufacturer's instructions (Qiagen, Hilden, Germany). RNA quality was assessed using spectrophotometric measurement with the Nanodrop 8000 (Labtech International) and Agilent Bioanalyser (Agilent, Santa Clara, CA). Total RNA (200 ng) was processed using the Applause-WT plus and the Encore Biotin module (NuGen, San Carlos, CA). Quality control of the amplified product was performed using the Nanodrop spectrophotometer and Agilent Bioanalyser. The amplified product was fragmented and labelled using the Encore Biotin module kit. All procedures strictly adhered to the manufacturers protocols. The labelled products were hybridized to GeneChip Exon WT arrays (Affymetrix, Santa Clara, CA). The Affymetrix 450 fluidics station and the Affymetrix 3000 G7 gene scanner were used to wash, stain and scan the arrays. Cell intensity calculation, scaling and quality control were performed using Affymetrix Expression Console. Statistical analysis and gene lists were generated using Partek Express (Partek, St.Louis. MI).

## References

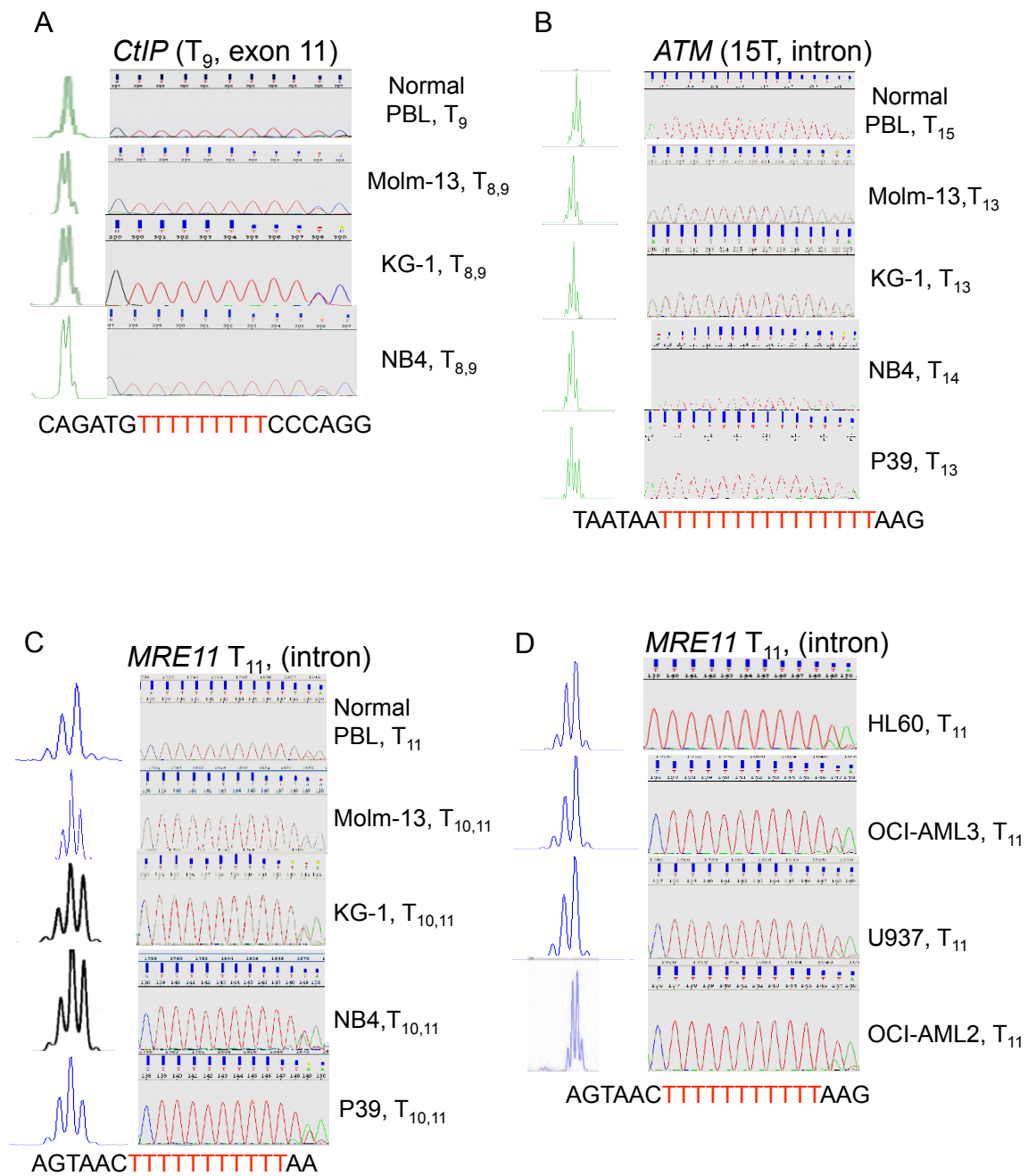
1. Jädersten M, Saft L, Smith A, Kulasekararaj A, Pomplun S, Göhring G, Hedlund A, Hast R, Schlegelberger B, Porwit A, Hellström-Lindberg E, Mufti GJ. TP53 mutations in low-risk myelodysplastic syndromes with del(5q) predict disease progression. *J Clin Oncol.* 2011;29:1971-9.
2. Plummer R, Jones C, Middleton M, Wilson R, Evans J, Olsen A, Curtin N, Boddy A, McHugh P, Newell D, *et al.* Phase 1 study of the poly(ADP-ribose) polymerase inhibitor, AG014699, in combination with temozolomide in patients with advanced solid tumors. *Clin. Can. Res.* 2008; 14:7917-7923.

Supplementary Figure S1



**Supplementary Figure S1. MSI profiling analysis in MDS/AML cell lines (A-B)** MSI loci profiles of MDS/AML cell line and normal PBL DNA using fluorescent fragment PCR for (A), NR21 and (B), BAT26 microsatellites. Arrows depict mean size of PCR product from normal PBL. Microsatellite sequence is shown under respective profile.

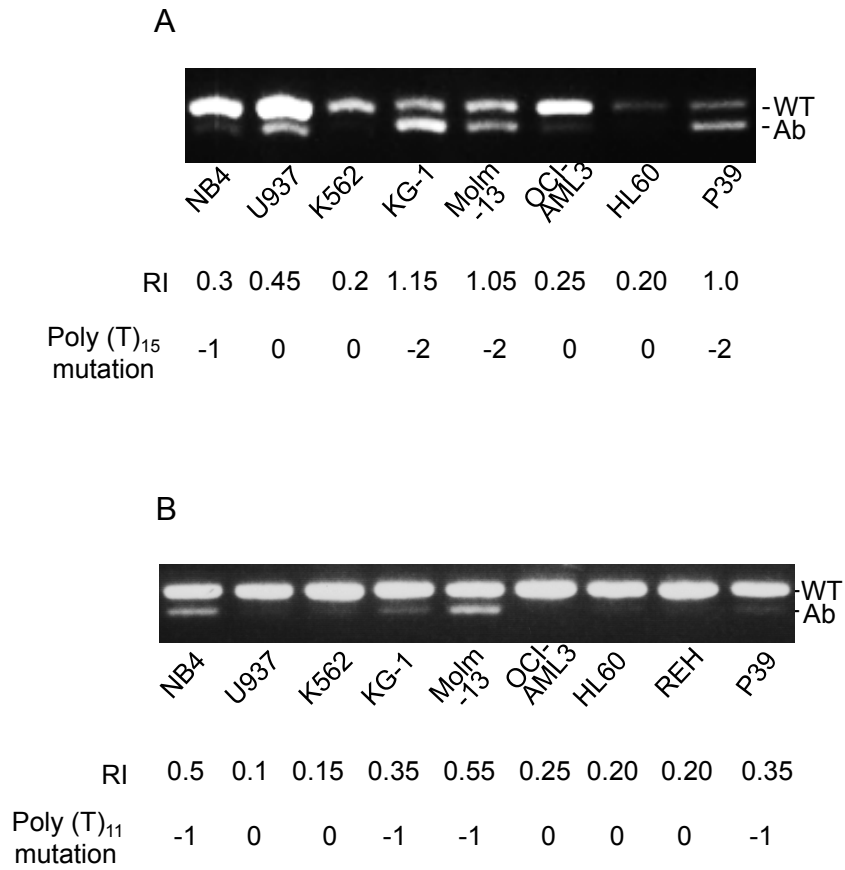
Supplementary Figure S2



**Supplementary Figure S2 Fluorescent fragment PCR and sanger sequencing of DNA repair gene coding region microsatellites.** (A-D), DNA from MDS/AML cell lines and normal PBL were used in PCR reactions for (A), *CtIP*, 9 thymine microsatellite ( $T_9$ , exon 11), (B), *ATM*, 15 thymine microsatellite ( $T_{15}$ , intronic) and (C-D) *MRE11*, 11 thymine ( $T_{11}$ , intronic). Fluorescent fragment profile is shown in left panel, sanger sequence is shown in right panel. Microsatellite sequence is shown under respective profile.

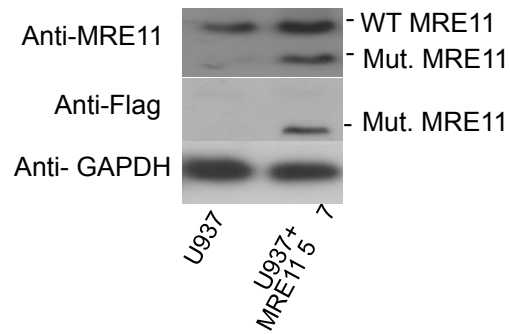


Supplementary Figure S3



**Supplementary Figure S3. Aberrant gene transcripts of *ATM* and *MRE11* in MDS/AML cell lines.** PCR amplification for (A), exon 8 of *ATM* and (B) exon 5 for *MRE11* were performed on cDNA from MDS/AML cell lines. Ratio of intensities (RI) between wild-type (WT) and aberrant (Ab) transcript were determined by measuring the intensity of gel bands using Adobe Photoshop™.

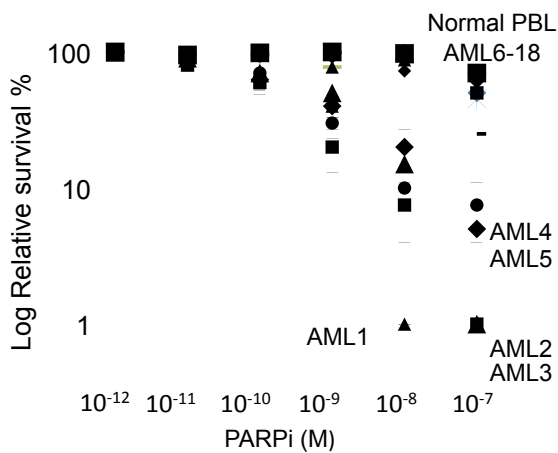
Supplementary Figure S4



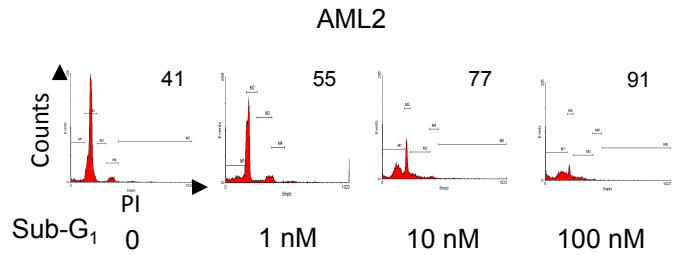
**Supplementary Figure S4** Mutant *MRE11* 5[Δ]7 in pIRESpURO3 was stably transfected into U937. *MRE11* 5[Δ]7 contains a C-terminal FLAG sequence and immunoblots were probed with anti-MRE11 and anti-FLAG.

## Supplementary Figure S5

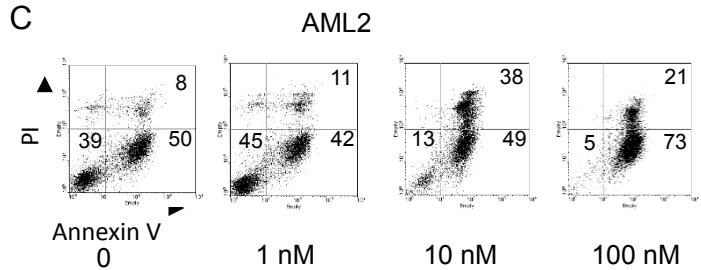
A



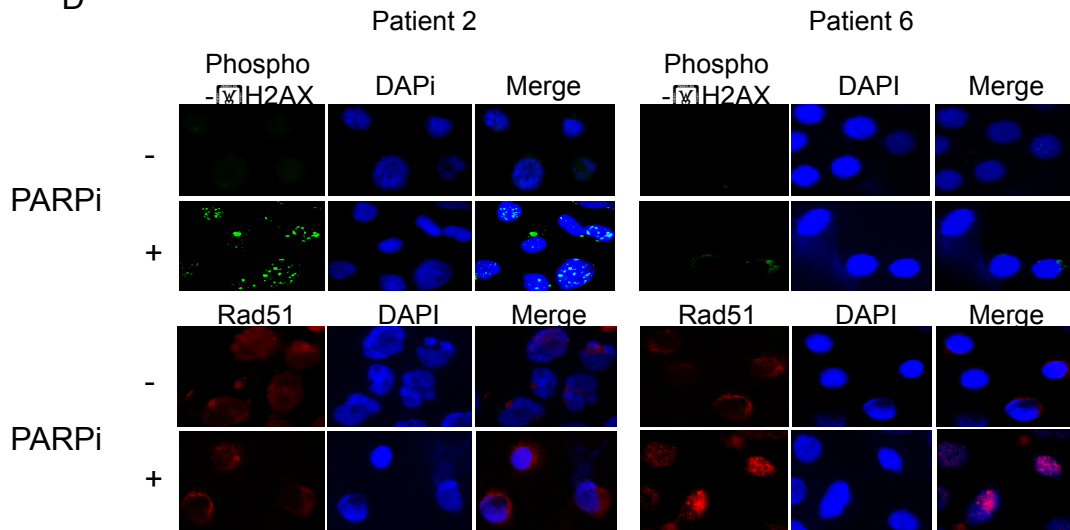
B



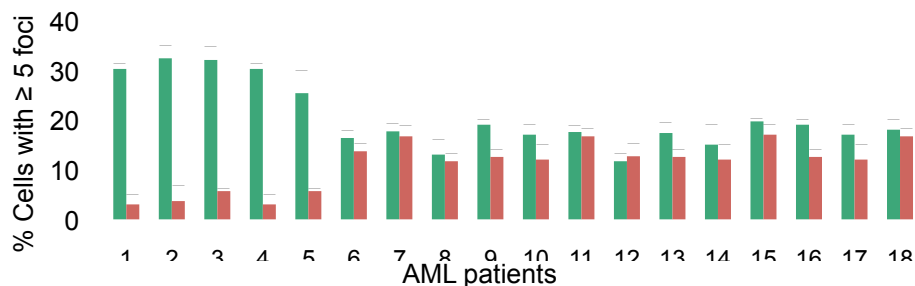
C



D

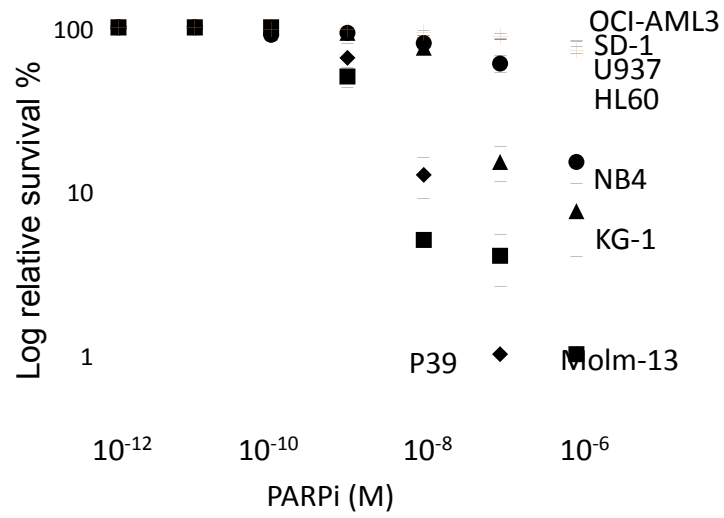


E



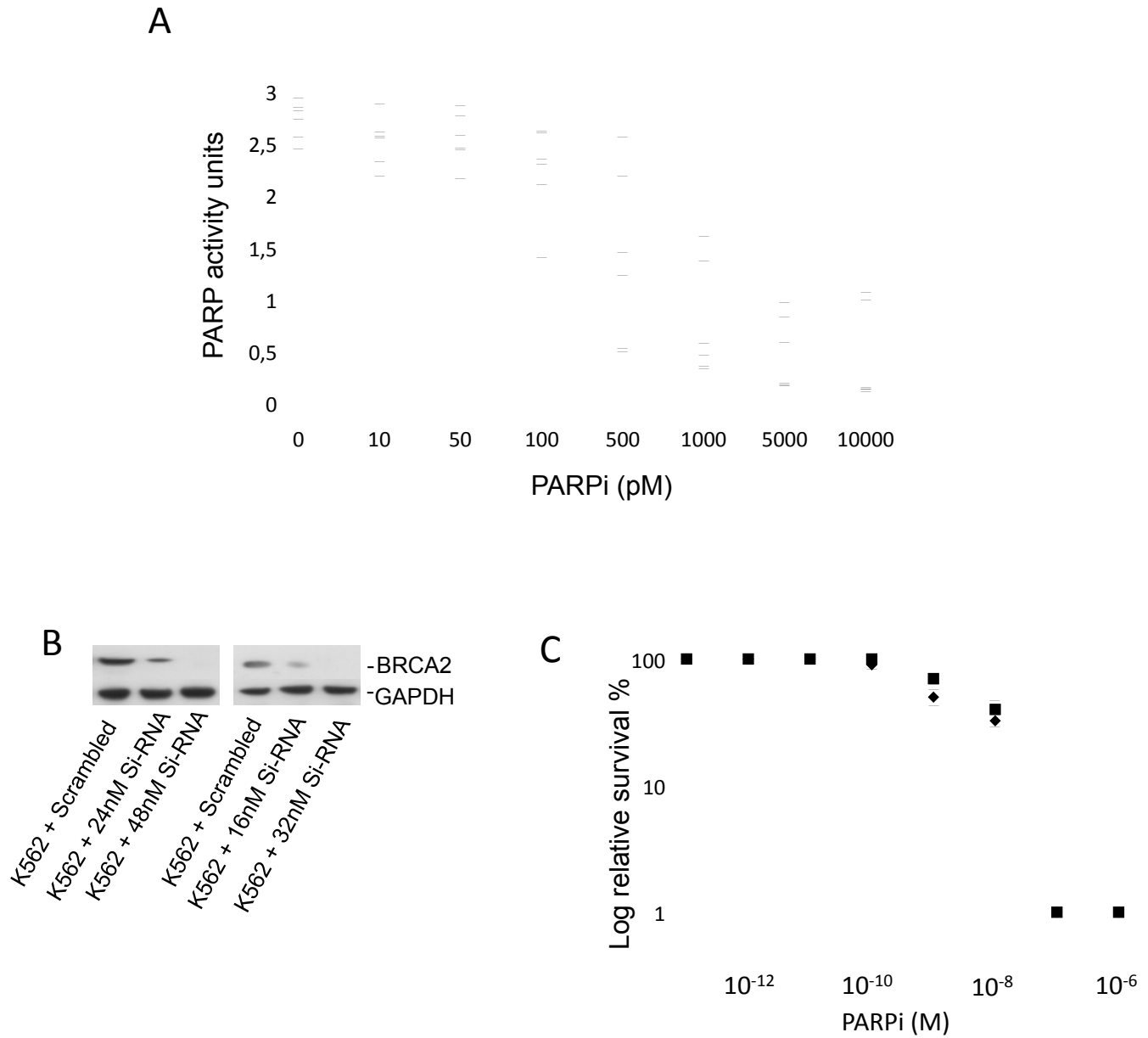
**Supplementary Figure S5 The effect of PARPi on primary AML cell survival.** (A). Viability analysis using trypan blue exclusion assays. Primary AML cells and normal peripheral blood lymphocytes (PBL) were cultured with increasing concentrations of PARPi continuously for 120 h. AML1 (open triangles), AML2 (solid squares), AML3 (solid triangles), AML4 (solid circles), AML5 (solid diamonds), AML6-18 and normal PBL (As indicated) (Error bars represent the means  $\pm$  S.E.M. of three separate experiments). (B), Analysis by flow cytometry. Increasing PARPi concentrations were added to AML patient 2 cells for 120 h. The apoptotic index (sub-G<sub>1</sub> population as a fraction of the total population, is shown right inset). (C), Analysis by Annexin V on the cell surface. Increasing concentrations of PARPi were added to AML patient 2 cells for 120 h before being treated with annexin V-FITC (FL-1, X-axis) and propidium iodide (PI) (FL-2, Y-axis). The figures show the percentage of non-apoptotic (bottom left quadrant), early (bottom right quadrant) and late apoptotic cells. (top right quadrant). D,E, DSB DNA repair by immunohistochemistry of rad51 and phospho- $\gamma$ H2AX foci. (D), Representative immunostaining of nuclei from primary AML cells treated with 100 nM PARPi for 24 h. Cells were probed for phospho- $\gamma$ H2AX or rad51 foci and nuclei were stained with DAPI. E, Frequency of cells displaying phospho- $\gamma$ H2AX foci (%) (green bars) or rad51 foci (%) (red bars), by immunofluorescence following PARPi addition in (B) primary AML and (C) MDS/AML cell lines. 200 nuclei were counted per experiment. Error bars represent the means  $\pm$  S.E.M. of three separate experiments.

Supplementary Figure S6



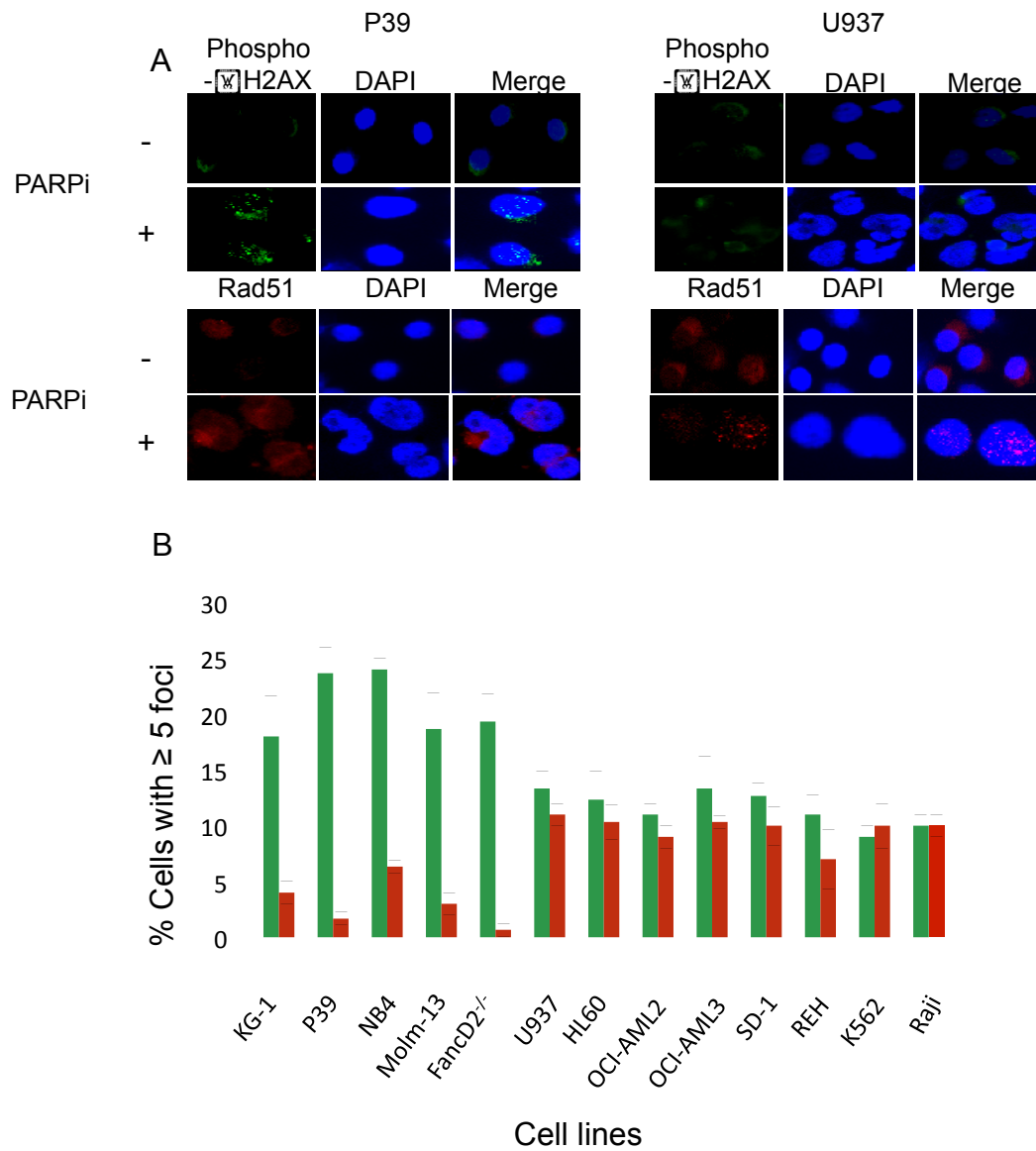
**Supplementary Figure S6. The effect of PARPi on MDS/AML cell line survival.** (A), Cell survival was assessed by soft agar clonogenic assay. Cells were exposed to variable concentrations of PARPi for 120 h before cloning in soft agar for a further 14 days. P39 (⊗), Molm-13 (■), KG-1 (▲), NB4 (●), OCI-AML3 (X), SD-1 (+), U937 (o), HL60 (\*)

Supplementary Figure S7



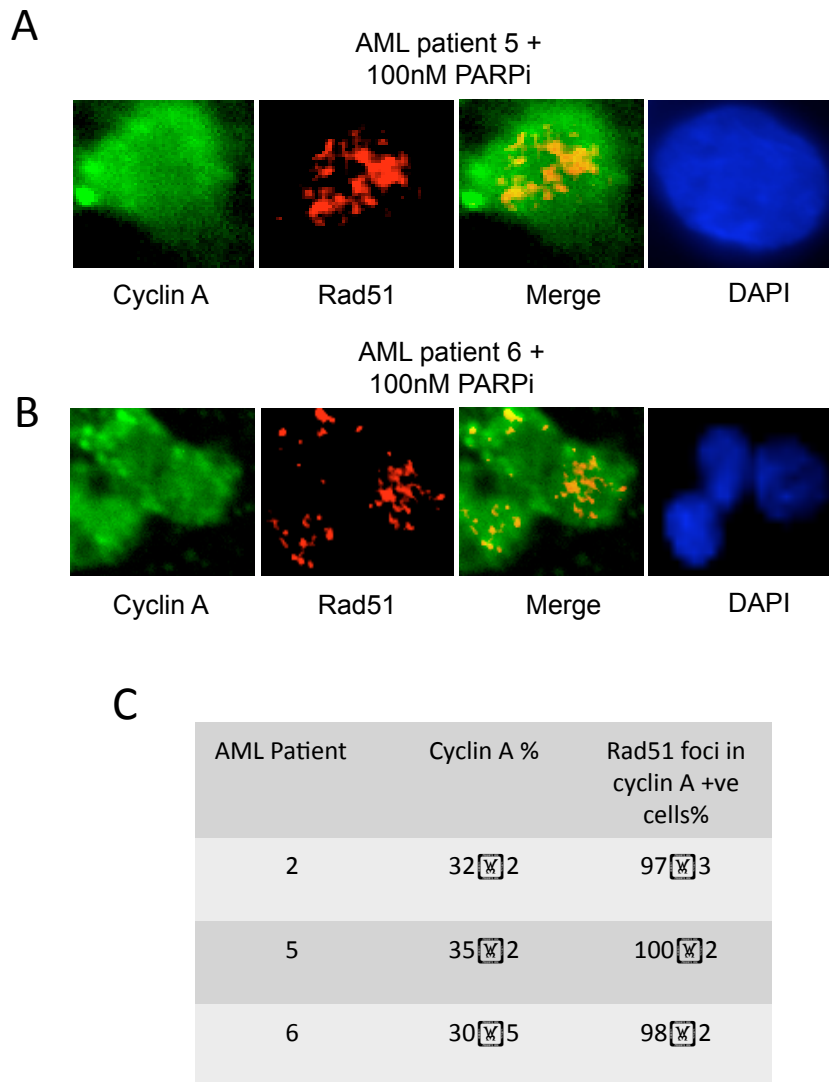
**Supplementary Figure S7. PARPi abrogation of PARP activity.** A. Comparison of PARPi. PARP enzyme activity assays using increasing concentrations of BMN 673 (blue), KU-0058948 (red) and PJ34 (green) were conducted as per manufacturer's instructions using nuclear extract from AML patient 2 cells as a source of PARP enzyme. B, K562 cells were transfected with BRCA2 Si-RNA (Dharmacon, left panels) and (Santa Cruz, right panels) using nucleofection. C, BRCA2 Si-RNA transfected K562 were treated with PARPi for a further 24h before cloning in soft agar for a further 14 days. BRCA2 Si-RNA (Dharmacon) (◻), BRCA2 Si-RNA (Santa Cruz) (◼).

Supplementary Figure S8



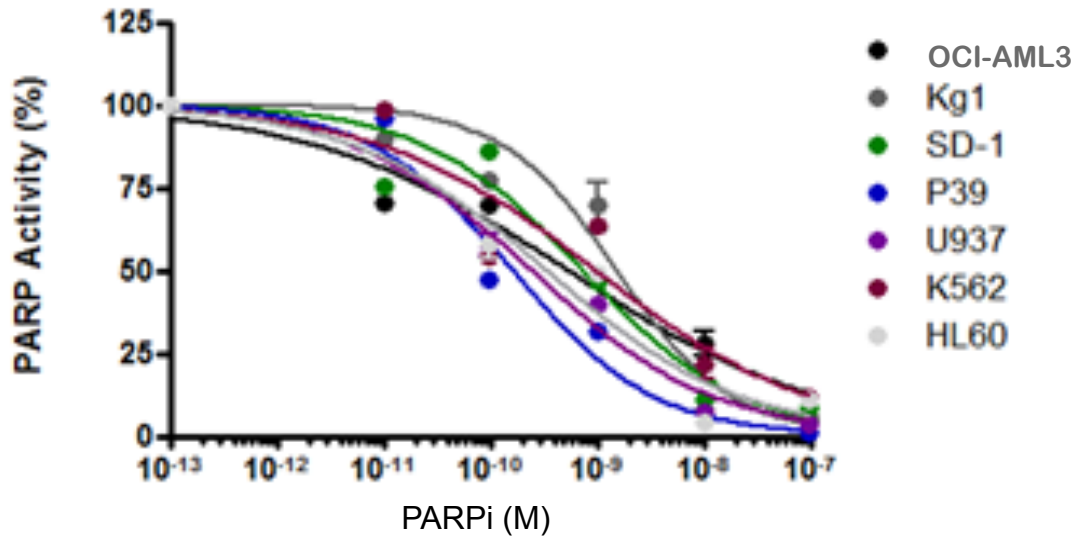
**Supplementary Figure S8 Immunostaining of nuclei from MDS/AML cell lines.** A, Cells were treated with 100 nM PARPi for 24 h in PARP sensitive P39 cells (left) and PARPi insensitive U937 (right). Representative foci from cells probed for phospho- $\gamma$ H2AX foci or rad51 foci and nuclei were stained with DAPI. B, Detection of frequency of cells displaying phospho- $\gamma$ H2AX foci (%) (green bars) or rad51 foci (%) (red bars), by immunofluorescence following PARPi addition. More than 200 nuclei were counted per experiment. Mean  $\pm$ S.E.M were determined in three separate experiments.

Supplementary Figure S9



**Supplementary Figure S9.** Mutant MRE11 and mutant CtIP do not affect cell cycle distribution of rad51 foci after DSB damage. A, Log phase AML patient 5 and 6 cells were treated with 100 nM PARPi for 24 h and immunostained for cyclin A, rad51 and counterstained with DAPI. Representative images are shown. B, Frequency of cells displaying cyclin A(%) or rad51 foci (%) (red bars), by immunofluorescence following PARPi addition in AML patients cells (n=3).

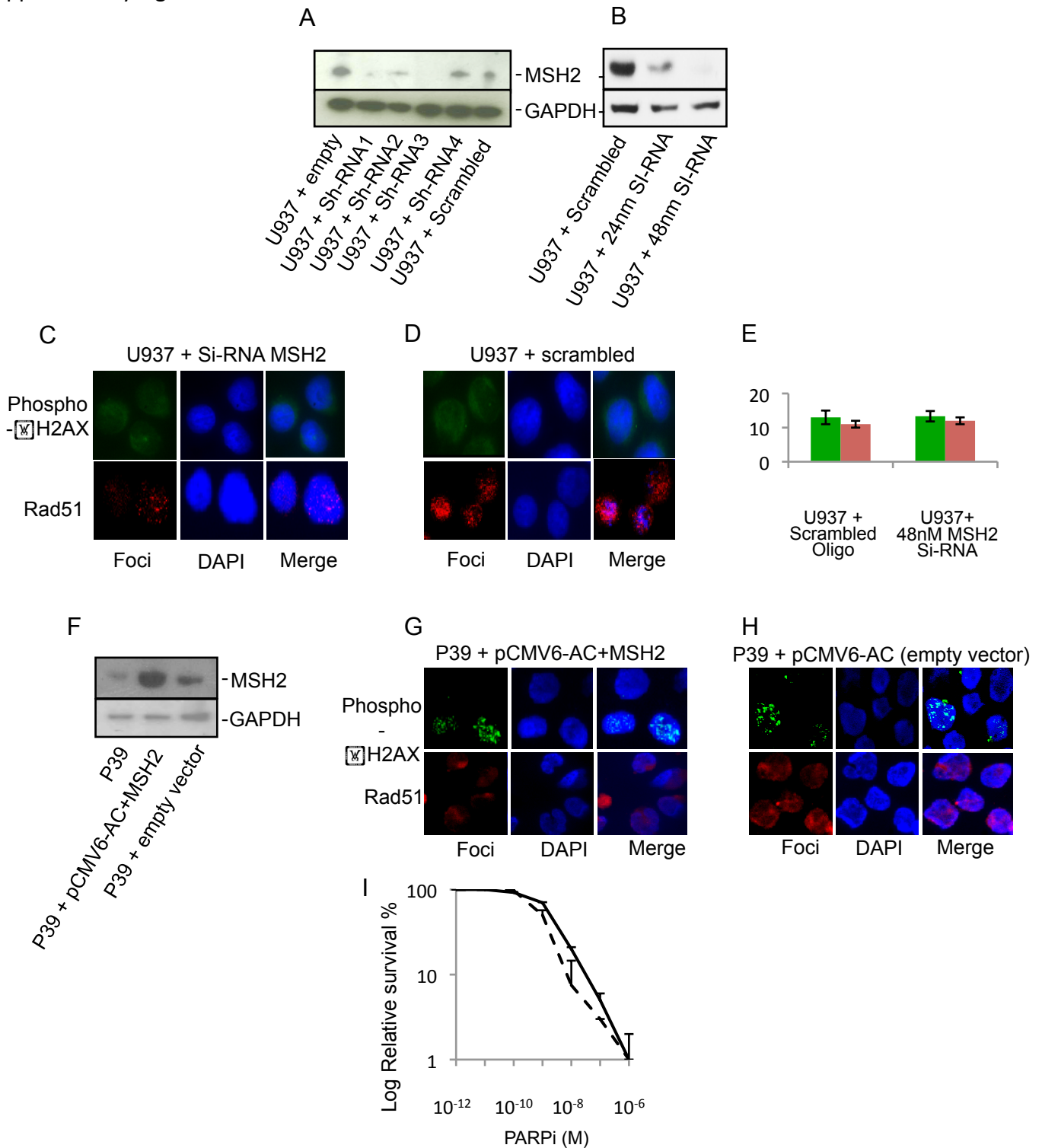
Supplementary Figure S10



**Supplementary Figure S10. Dose response curves of intrinsic PARP activity in MDS/AML cell lines.** Dose response curves of intrinsic PARP activity in MDS/AML cell lines. Increasing PARPi concentration was added to cells prior to the determination of PAR accumulation. Cells were stimulated by exposing permeabilised cells to blunt-ended oligonucleotide in the presence of NAD<sup>+</sup>.

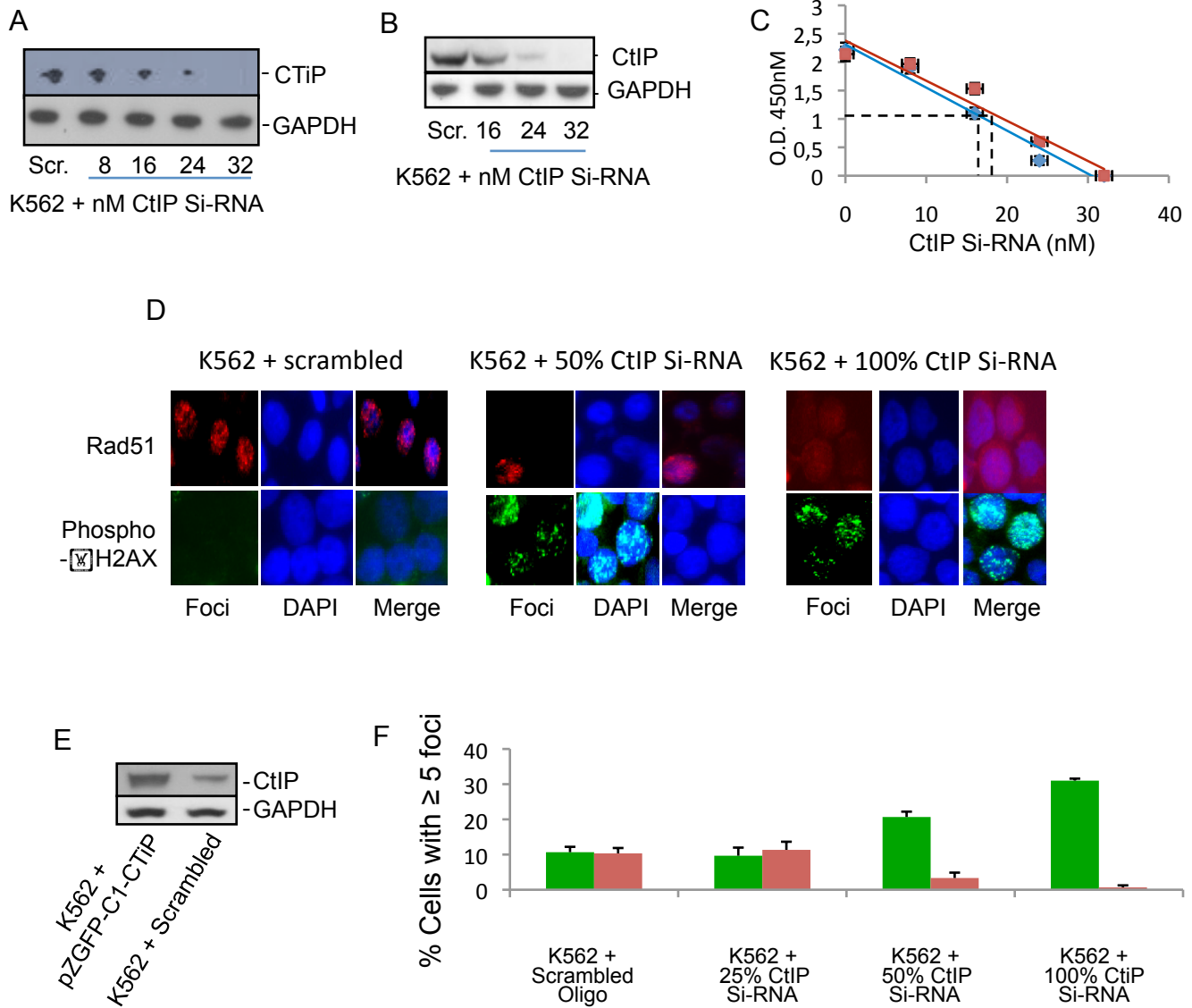


Supplementary Figure S11



**Supplementary Figure S11. Modulation of MMR.** A,B Immunoblots were prepared from whole cell extracts of U937 cells transfected with A, SH-RNA vectors (SH-RNA 1-4) and B, Si-RNA to MSH2. Scrambled oligonucleotides acted as silencing controls for Sh-RNA and Si-RNA. Immunoblots were probed with anti-MSH2 and anti-GAPDH. C,D Representative immunostaining of nuclei from C, U937 + Si-RNA MSH2 and D, U937 + scrambled oligo control, pre-treated with 100nM PARPi for 24 h. E, Frequency of cells displaying phospho- $\gamma$ H2AX foci (%) (green bars) or rad51 foci (%) (red bars), by immunofluorescence following PARPi addition in MSH2 Si-RNA depleted cells and scrambled oligo. controls. 200 nuclei were counted per experiment. Error bars represent the means  $\pm$  S.E.M. of three separate experiments. F-I, Over-expression of MSH2. F, pCMV6-AC + MSH2 sequence was stably transfected into P39 cells. Immunoblots were probed with anti-MSH2 and anti-GAPDH. G-I, Representative immunostaining of nuclei from G, P39 + pCMV6-AC+MSH2 (over-expressed MSH2) and H, P39 + pCMV6-AC (empty vector) pre-treated with 100nM PARPi for 24 h. I, P39 + pCMV6-AC+MSH2 (over-expressed MSH2, solid line), P39 + pCMV6-AC (empty vector, dashed line) PARPi was incubated for 120 h before plating on soft agar for 14 days.

Supplementary Figure S12



**Supplementary Figure S12** A-B Increasing concentrations of Si-RNA (A, Dharmacon, B, Santa Cruz) to CtIP were transfected into K562 by nucleofection and immunoblots probed with anti-CtIP. Scrambled oligonucleotides acted as a silencing control. C, ELISA standard curve prepared of increasing concentrations of Si-RNA (Dharmacon, blue diamonds), B, Santa Cruz, red squares) to CtIP transfected into K562 by nucleofection. Extracts were prepared and ELISA for CtIP expression was performed. Dotted line interpolates the concentration of si-RNA to give 50% of CtIP expression. D, Representative rad51 and phospho- $\gamma$ H2AX foci after treatment with 100 nM PARPi for 24 h in K562 + scrambled oligo (left panel), 50% (19nM) CtIP Si-RNA (Santa Cruz, Center panel), and K562 + 100% (32nM) CtIP Si-RNA (right panel) E, Over-expression of CtIP. K562 was transfected with the CtIP over-expressing plasmid, pZGFP-C1-CtIP or with a scrambled oligonucleotide control. F, Frequency of phospho- $\gamma$ H2AX foci positive cells (%) (green bars) and rad51 foci positive cells (%) (red bars) following 24 h PARPi addition. Error bars represent the means  $\pm$  S.E.M. of three separate experiments.

Supplementary Table S1 Clinical and Cytogenetic information for the AML patient cohort. BM – Bone marrow, PB – Peripheral Blood.

Patient	Sample	FAB	Cytogenetics
AML 1	No Data	No Data	No data
AML 2	BM	M2 (tAML)	t(6;10)(q27;q21)[5]/46,XY,del(1)(q25q32),add(4)(q35)
AML 3	BM	M5	Failed
AML 4	PB	CML→AML M4	Failed
AML 5	BM	M1	+4,t(6;9)(p23;q34),t(15;17)(q15;q11)
AML 6	PB	MDS/AML M4	Normal
AML 7	PB	M2	Normal
AML 8	BM	M4	Normal
AML 9	BM	M5	Normal
AML 10	BM	M5	+8
AML 11	BM	M5	+4, +8, +21
AML 12	BM	MDS-AML M4	-7
AML 13	BM	M6	Normal
AML 14	No Data	No Data	No data
AML 15	No Data	No Data	No data
AML 16	No Data	No Data	No data
AML 17	No Data	No Data	No data
AML 18	No Data	No Data	No data





**Supplementary Table S4 Intrinsic PARP activity of MDS/AML cell lines.** Cells were stimulated by exposing permeabilised cells to blunt-ended oligonucleotide in the presence of NAD<sup>+</sup>.

MDS/AML cell line	Basal unstimulated PAR (nmol) per 10 <sup>6</sup> cells	Basal stimulated PAR (nmol) per 10 <sup>6</sup> cells	PARPi Sensitivity
P39	1.3	39.2	++
KG1	1.7	84.7	+
SD-1	1.1	30.8	-
OCI-AML3	1.6	57.3	-
U937	1.2	58.8	-
K562	1.6	43.2	-
HL60	0.3	29.4	-

Supplementary Table S5

**Supplementary Table S5. Chromosomal locations and aberrations in 63 high risk MDS patient determined by SNP analysis.** For MSI, L=MSI-low, H=MSI-high and N=negative. For TP53, WT = wild type, Mut. = Mutated. For Type, LOH = copy neutral loss of heterozygosity, (LOH)/UPD, NA = No aberrations. Therapy related MDS (t-MDS) patients are indicated by an asterisk (\*).

MDS patient	MSI	TP53	Type	Chromosome	Cytoband Start	Cytoband End	Size (bp)
1	L	WT	LOH	11	q12.3	q25	72,246,167
2	H	WT	LOH	2	p25.3	p16.3	46,931,070
			Loss	5	q23.1	q32	28,599,727
			Loss	7	p22.3	q36.3	156,256,445
3	L	WT	LOH	11	q13.1	q25	67,782,871
4	L	WT	LOH	7	q22.1	q36.3	57,408,500
5	H	Mut.	Loss	1	q24.2	q24.2	3,326,516
			Loss	1	q42.13	q42.3	7,483,492
			Loss	4	q21.23	q35.2	105,967,537
			Loss	5	q33.2	q33.2	340,119
			Loss	5	q31.3	q31.3	445,640
			Loss	5	q14.3	q15	3,399,516
			Loss	5	q23.2	q31.2	12,587,265
			Loss	7	p22.3	q36.3	158,604,880
			Loss	12	p11.22	q12	12,065,388
			Loss	12	p13.33	p12.1	20,011,424
			Loss	12	q21.1	q24.33	61,384,780
			Loss	16	p13.3	q24.3	88,301,897
			Loss	17	p13.3	p11.2	19,127,603
			Loss	20	q11.22	q13.33	26,051,760
			Loss	21	q11.2	q21.2	9,398,158
6	L	Mut	Loss	7	q11.23	q36.3	81,592,379
			Gain	9	p24.3	p12	40,543,174
			Loss	9	q13	q34.3	70,071,368
			Loss	18	q22.1	q22.1	839,580
			Gain	18	q21.1	q21.1	853,313
			Gain	18	q12.1	q12.1	916,710
			Gain	18	q12.3	q12.3	1,082,691
			Gain	18	q21.1	q21.1	1,851,938
			Loss	18	q22.3	q23	3,641,787
			Gain	18	q22.1	q22.3	7,209,487
			Gain	18	q21.2	q22.1	14,562,004
			Gain	20	q13.31	q13.33	6,023,652
			Gain	20	q13.2	q13.33	8,459,277
			Loss	21	q21.1	q21.1	2,034,128
			Loss	21	q21.1	q21.3	5,063,530
			Loss	21	q22.11	q22.13	6,523,769
			Gain	21	q22.13	q22.3	9,862,454
7	H	WT	Gain	1	q21.3	q44	96,150,471
			Loss	6	q14.1	q14.1	1,662,513
			Loss	7	q11.22	q31.33	58,583,639
			Gain	9	p24.3	q12	69,231,244

Supplementary Table S5

<b>8</b>	L	WT	LOH	20	q11.21	q13.33	32,606,676
			Loss	21	q22.12	q22.12	952,246
<b>9</b>	L	WT	LOH	6	p22.2	p21.32	7,289,924
			Loss	7	q22.1	q36.3	59,221,010
			Gain	9	p24.3	p13.1	37,563,330
<b>10</b>	L	WT	Gain	3	q23	q29	55,618,436
			Loss	7	p22.3	p14.2	35,421,613
			Loss	18	p11.32	p11	14,859,205
			Loss	18	q21	q23	24,989,855
			Gain	18	q11.1	q21.2	34,300,911
<b>11</b>	H	WT	LOH	21	q21.3	q22.3	
			LOH	2	p14	p12	10,988,646
			LOH	4	q31.22	q31.3	7,196,190
			LOH	9	p21.2	p13.2	11,110,432
			LOH	19	q12	q13.2	7,684,988
<b>12*</b>	L	WT	Loss	7	p22.3	q36.3	158,409,722
			LOH	13	q12.13	q34	87,664,433
<b>13*</b>	L	Mut.	Loss	6	p21.32	p21.32	429,074
			Loss	6	p21.1	p21.1	1,345,937
			Gain	6	p21.31	p21.2	3,743,048
			Loss	6	p23	p22.1	11,577,909
			Loss	6	p25.3	p23	13,937,899
			Loss	7	p14.1	q36.3	118,980,258
			Gain	18	q21.1	q21.2	1,445,313
			Loss	18	q21.1	q21.1	1,760,639
			Loss	18	q21.31	q21.32	2,568,307
			Loss	18	q22.1	q23	15,448,142
<b>14</b>	N	WT	Gain	18	q11.1	q21.1	26,380,056
			Loss	21	q22.11	q22.12	1,032,303
			NA	NA	NA	NA	NA
			NA	NA	NA	NA	NA
<b>15</b>	N	WT	NA	NA	NA	NA	NA
<b>16</b>	N	WT	NA	NA	NA	NA	NA
<b>17</b>	N	WT	NA	NA	NA	NA	NA
<b>18</b>	N	WT	loss	X	p11.4	p11.4	2,410,192
			loss	3	q26.2	q26.2	403,464
<b>19</b>	N	Mut.	Loss	5	q31.2	q35.3	42,795,999
			Gain	17	q24.3	q24.3	589,218
			Gain	17	q23.2	q23.3	665,042
			Gain	17	q24.2	q24.2	1,561,077
			Loss	17	q24.3	q25.1	1,714,932
			Gain	17	q25.2	q25.2	1,874,682
			Loss	17	q24.2	q24.3	2,186,420
<b>20</b>	N	WT	Loss	17	p13.3	p13.1	10,228,035
			Loss	17	p13.1	p11.2	11,089,216
			Loss	11	p15.5	p15.4	1,101,866
<b>21</b>	N	WT	NA	NA	NA	NA	NA



Supplementary Table S5

<b>22</b>	N	WT	Gain	1	p32.3	p32.3	832,764
			Gain	1	p35.1	p34.1	12,694,360
			Loss	1	p36.33	p35.2	31,041,095
			Loss	5	p15.33	p11	42,345,754
			Loss	5	q14.3	q35.3	97,686,987
			Gain	7	q21.2	q21.3	4,909,738
			Loss	7	q22.1	q33	37,306,046
			Gain	17	p13.1	p12	4,762,509
			Loss	17	q21.33	q22	5,384,700
			Gain	17	p11.2	q11.1	5,742,949
			Gain	17	q22	q23.2	5,978,707
			Loss	17	q11.2	q12	8,740,685
			Loss	17	p13.3	p13.1	8,979,444
			Loss	17	q24.3	q25.3	10,227,513
<b>23</b>	N	WT	Gain	21	q22.13	q22.3	9,186,979
			Loss	5	q31.2	q31.2	990,832
			Loss	5	q13.3	q13.3	1,126,845
			Gain	11	q13.4	q25	61,270,945
<b>24</b>	N	Mut.	Loss	17	q11.2	q11.2	2,457,176
			Loss	5	q11.1	q35.3	131,161,016
			Loss	6	p21.31	p21.31	1,477,361
			Gain	6	p21.31	p21.2	2,160,378
			Loss	6	p21.2	p21.1	2,714,594
			Gain	6	p21.1	p12.3	6,042,249
			Gain	6	p22.2	p21.31	9,685,287
			Loss	6	p25.3	p22.2	25,238,463
			Loss	7	p12.1	p12.1	270,872
			Loss	7	q22.1	q22.1	1,739,336
			Gain	7	p15.2	p14.3	7,908,955
			Loss	7	p14.3	p12.1	18,664,719
			Loss	7	p22.3	p15.2	26,258,663
			Gain	7	p12.1	q22.1	47,000,330
<b>25</b>	N	WT	Gain	15	q22.31	q26.3	38,010,049
			Loss	15	q11.2	q22.31	39,979,291
			Gain	19	q12	q13.43	31,028,595
			Loss	7	p22.3	q36.3	158,805,161
			Loss	12	p13.2	p13.1	1,621,380
			<b>26</b>	N	WT	Loss	7
LOH	17	q21.32				q25.3	36,053,322
<b>27</b>	N	WT	NA	NA	NA	NA	NA
<b>28</b>	N	Mut.	Loss	5	p15.33	p14.3	22,354,035
			Loss	5	q11.2	q33.3	108,844,776
			Loss	17	p13.3	p11.2	16,201,282
			Gain	19	q12	q13.43	30,772,620
<b>29</b>	N	Mut.	Loss	1	q21.3	q24.2	6,358,346
			Gain	1	p36.33	q21.3	150,237,257

Supplementary Table S5

<b>29</b>	N	Mut.	Loss	3	p21.1	q13.13	58,719,043
			Loss	5	q11.2	q35.3	126,174,982
			Gain	7	q21.13	q21.13	1,475,518
			Gain	7	q21.3	q22.1	2,266,285
			Gain	7	q21.11	q21.11	3,429,101
			Loss	7	q22.1	q36.1	51,383,635
			Loss	11	p12	p12	3,765,499
			Loss	18	p11.32	p11.21	12,593,432
			Loss	18	q12.1	q23	52,578,994
			Gain	19	p13.3	p13.11	11,377,279
			Loss	21	q22.3	q22.3	2,140,795
			<b>30</b>	N	WT	NA	NA
<b>31</b>	N	WT	Loss	7	p22.3	q36.3	158,604,880
<b>32</b>	N	WT	NA	NA	NA	NA	NA
<b>33</b>	N	Mut.	Loss	3	q26.2	q26.2	474,136
			Loss	3	q21.3	q21.3	1,211,973
			Loss	7	q21.3	q36.3	68,868,000
			Loss	7	p22.3	p11.2	58,761,999
<b>34</b>	N	WT	NA	NA	NA	NA	NA
<b>35</b>	N	WT	Gain	8	p23.3	q24.3	146,268,948
			Loss	21	q22.12	q22.12	1,202,318
<b>36</b>	N	Mut.	Loss	3	p25.2	p24.3	6,713,571
			Gain	3	q25.2	q29	43,928,347
			Loss	5	q11.1	q12.1	13,048,970
			Loss	5	q12.2	q35.3	117,332,202
			Loss	7	p11.2	q36.3	103,799,684
			Gain	11	q23.1	q25	37,876,450
			Loss	13	q12.3	q21.33	37,613,578
			Loss	18	p11.31	p11.21	7,449,195
			Loss	18	q22.2	q23	11,592,865
			Loss	20	p13	p13	1,317,978
<b>37</b>	N	WT	Loss	20	q11.23	q13.32	21,084,879
			Gain	X	p22.33	q13.1	70,951,090
			Loss	X	q13.1	q28	82,862,904
<b>38</b>	N	WT	Loss	7	p22.3	q36.3	156,690,906
<b>39</b>	N	WT	NA	NA	NA	NA	NA
<b>40</b>	N	WT	Loss	7	q21.11	q36.3	71,620,655
<b>41</b>	N	Mut.	Loss	2	p25.1	p23.3	15,116,825
			Loss	5	q15	q34	67,728,653
			Loss	7	q11.21	q36.3	92,942,222
			Gain	8	p23.3	q24.3	145,619,410
			Gain	12	p12.3	p12.3	761,314
			Loss	12	p13.33	p13.33	2,442,057
			Gain	12	p13.33	p13.31	2,941,334
			Gain	12	p12.2	p12.1	5,550,278
Loss	12	p13.31	p12.3	12,957,571			

Supplementary Table S5

<b>41*</b>	N	Mut.	Gain	13	q13.3	q14.11	22,256,520
			Loss	16	q21	q24.3	30,151,806
			Loss	17	p13.3	p13.1	6,890,047
			LOH	17	p13.1	p11.2	9,938,138
			Loss	20	q11.22	q12	8,340,967
			Gain	X	p22.33	q13.2	72,105,045
<b>42</b>	N	WT	Loss	X	q13.2	q28	82,618,613
<b>43</b>	N	WT	NA	NA	NA	NA	NA
<b>44</b>	N	WT	NA	NA	NA	NA	NA
<b>45*</b>	N	Mut.	LOH	1	q32.1	q44	44,251,250
			Loss	2	p23.3	p23.3	894,368
			Loss	5	q13.2	q13.3	988,421
			Loss	5	q13.3	q35.3	105,364,002
			Gain	6	p25.3	q27	170,013,200
			Loss	7	q11.22	q36.3	88,629,175
			Gain	8	p23.3	q24.3	145,358,662
			Loss	11	p15.5	p15.4	2,194,893
			Gain	11	p15.4	q25	11,048,675
			LOH	11	q13.3	q24.1	53,306,391
			Gain	12	p13.33	p13.32	8,365,844
			Loss	12	p13.31	p11.21	21,491,742
			Gain	13	q11	q34	96,047,764
			Loss	16	q12.1	q21	7,042,932
			Loss	16	q23.1	q24.3	14,261,151
			<b>46</b>	N	Mut.	LOH	17
Loss	5	q12.3				q13.1	2,502,865
Loss	5	q14.1				q35.3	99,891,001
LOH	6	q16.1				q21	10,513,792
Loss	7	q11.23				q36.3	83,878,779
Gain	11	q21				q25	39,784,438
Loss	12	p13.32				p12.3	12,373,525
LOH	17	p13.3				p11.2	20,861,790
Loss	18	q21.2				q23	29,282,490
Loss	18	p11.31				q21.2	43,624,224
<b>47</b>	N	WT	NA	NA	NA	NA	NA
<b>48</b>	N	Mut.	LOH	1	p33	p32.1	11,398,167
			Gain	1	p32.1	p13.3	49,134,561
			Gain	1	p36.33	p32.3	52,408,141
			Loss	3	q13.33	q21.3	5,915,046
			Loss	3	p24.3	p24.1	5,959,345
			Loss	3	p22.2	p21.32	89,081,713
			Loss	5	q13.2	q14.1	6,968,612
			Loss	5	q11.2	q12.1	7,276,891
			Loss	5	q23.3	q34	33,246,379
			Gain	5	p15.33	q11.2	50,836,922
Loss	7	p14.2	p14.1	4,470,952			

Supplementary Table S5

<b>48</b>	N	Mut.	Gain	8	p23.2	q24.3	144,708,552
			Gain	9	q32	q34.3	21,626,846
			Gain	9	p24.3	p13.2	36,866,488
			Gain	11	p15.4	q25	134,449,983
			Gain	17	p13.3	p13.2	4,345,750
			Loss	17	q11.2	q12	4,997,615
			Loss	17	p13.2	p12	7,554,771
			Gain	22	q11.1	q13.33	34,678,319
<b>49</b>	N	WT	Gain	3	q23	q29	55,618,436
			Loss	7	p22.3	p14.2	35,421,613
			Loss	18	p11.32	p11	14,859,205
			Loss	18	q21	q23	24,989,855
			Gain	18	q11.1	q21.2	34,300,911
			LOH	21	q21.3	q22.3	
<b>50</b>	N	WT	Loss	7	p22.3	q36.3	158,805,161
<b>51</b>	N	WT	Loss	7	p22.3	q36.3	158,752,262
<b>52</b>	N	WT	NA	NA	NA	NA	NA
<b>53</b>	N	WT	NA	NA	NA	NA	NA
<b>54</b>	N	WT	NA	NA	NA	NA	NA
<b>55</b>	N	WT	Loss	2	p24.1	p23.3	3,297,060
			Loss	7	p22.3	p11.2	55,934,904
			Loss	7	q21.13	q36.3	67,965,029
			Loss	11	q22.3	q22.3	4,516,506
			Loss	11	q14.1	q14.1	5,744,116
			Loss	11	q14.3	q22.3	11,631,889
			Loss	12	q12	q12	4,921,459
			Loss	12	q21.32	q23.1	10,976,489
			Loss	12	p13.2	p11.1	23,704,288
<b>56</b>	N	WT	Loss	7	p22.3	q36.3	157,920,856
<b>57</b>	N	WT	NA	NA	NA	NA	NA
<b>58</b>	N	Mut.	Gain	3	q23	q29	58,434,963
			Loss	5	q11.2	q33.3	98,798,227
			Loss	7	q22.1	q36.3	58,934,837
			Gain	8	p23.3	q24.3	145,677,905
			Loss	20	q11.21	q13.2	19,615,525
<b>59*</b>	N	Mut.	Loss	3	q13.13	q21.1	14,861,617
			Loss	5	q15	q35.3	83,791,337
			Loss	7	p22.3	q36.3	158,733,375
			Loss	11	p15.4	p15.4	295,125
			Loss	12	q13.13	q13.13	1,463,962
			Loss	12	p13.31	p12.1	15,395,354
			Loss	14	q24.2	q24.3	2,256,796
			Loss	18	q12.1	q23	50,284,979
			Loss	21	q11.2	q21.1	5,178,668
<b>60</b>	N	WT	Gain	8	p23.3	q24.3	146,138,089
			Gain	21	p11.2	q22.3	37,162,644

Supplementary Table S5

<b>61</b>	N	WT	Loss	17	p13.3	p11.2	18,722,403
			Gain	17	p11.2	q25.3	59,621,574
<b>62</b>	N	Mut.	Gain	4	q22.1	q22.1	843,051
			Gain	20	q13.32	q13.33	5,927,727
			Loss	20	p13	p11.1	25,693,546
			Loss	20	q11.21	q13.32	25,984,652
<b>63</b>	N	WT	Loss	7	q22.1	q36.1	44,986,591